Published in final edited form as:
Invest Radiol. 2008 May ; 43(5): 322–329. doi:10.1097/RLI.0b013e318168c715.

Acoustic Attenuation by Contrast Agent Microbubbles in Superficial Tissue Markedly Diminishes Petechiae Bioeffects in Deep Tissue

Ji Song, PhD[*], **Alexander L. Klibanov, PhD**[†], **John A. Hossack, PhD**[*], and **Richard J. Price, PhD**[*]

[*]Department of Biomedical Engineering, University of Virginia, Charlottesville, Virginia.

[†]Cardiovascular Division, University of Virginia, Charlottesville, Virginia.

Abstract

Objective—To measure how ultrasound attenuation by contrast agent microbubbles (MBs) in superficial tissue affects petechiae creation in underlying deep tissue.

Materials and Methods—Studies using Sprague-Dawley rats were approved by the Animal Care and Use Committee. MBs were injected intravenously, and 12 ultrasound pulses (100 sinusoids of 1 MHz ultrasound per pulse) were applied through the skin overlying the hindlimb adductors at intervals of 10 or 60 seconds. In some groups, the skin was resected and immediately returned without re-establishing vascular connections. Muscle petechiae were counted.

Results—Applying ultrasound through unperfused skin after bolus and continuous intravenous MB injection yielded, respectively, 30-fold and 3.5-fold more petechiae than for perfused skin. Surprisingly, petechiae/mm^2 decreased with a higher MB dosage [0.12 ±0.05 (1×10^5 MBs/g) vs. 0.04 ± 0.02 (3×10^5 MBs/g)] when ultrasound was applied through perfused skin. In contrast, petechiae/mm^2 was approximately proportional to MB dosage for unperfused skin [0.17 ± 0.10 (1×10^5 MBs/g) vs. 0.42 + 0.14 (3×10^5 MBs/g)]. In comparison to MB-free controls, MB solutions in this concentration range reduced the peak-negative pressure of ultrasound by 65% to 85%.

Conclusions—Acoustic attenuation by MBs in skin markedly reduces petechiae creation in deep muscle. Petechiae inhibition is dependent on $[MB]^{2.1}$ and, therefore, dominates the otherwise proportional relationship between petechiae and [MB] in muscle. The drop of peak-negative pressure below a critical microvessel rupturing threshold is the probable mechanism for petechiae inhibition. These results indicate that high MB doses could, paradoxically, reduce the potential for petechiae creation and may have important bearing on the design of contrast ultrasound-based therapeutics.

Keywords

ultrasound; microbubbles; contrast media; bioeffects; microcirculation

Injectable microbubble (MB) formulations enhance contrast between tissues during diagnostic ultrasound imaging,[1–3] permit the measurement of tissue perfusion,[4,5] and facilitate drug and gene delivery[6–12] and the direct stimulation of therapeutic arteriogenesis.[13–17] These therapeutic applications are often made possible by the ability of MBs to create pores in

Reprints: Richard J. Price, PhD, Department of Biomedical Engineering, University of Virginia, Box 800759, Health System, 415 Lane Road, MR5, Charlottesville, VA 22908. E-mail: E-mail: rprice@virginia.edu.

capillary walls when they are destroyed by ultrasound. [18–21] In some cases, these pores may be large enough to permit the extravasation of erythrocytes into tissue (ie, petechiae). This "petechiae bioeffect" phenomenon has also raised concerns about the clinical safety of contrast ultrasound. [22–25]

The creation of petechiae bioeffects is dependent on ultrasound power[18–20,22,24] and pulsing interval.[26] Modeling studies predict that increasing peak-negative acoustic pressure from 0.2 to 0.5 MPa increases the level of microvessel wall stress caused by MB expansion by 2 orders of magnitude, to a value above the critical threshold for vessel rupturing. [27] MB concentration ([MB]) also influences petechiae bioeffect creation, with petechiae creation being proportional to [MB] at low doses.[19,24] With regard to petechiae creation, 1 factor that has not been explored experimentally is MB self-attenuation, which is a complicating factor in contrast ultrasound imaging[28] and perfusion measurements.[29] Acoustic attenuation by MBs could, for example, explain why petechiae bioeffect creation eventually reaches a maximum, even as systemic [MB] continues to increase.[19] The purpose of this study was to test the hypothesis that acoustic attenuation, created by MBs in superficial tissue, significantly inhibits the creation of petechiae bioeffects in deep tissue.

MATERIALS AND METHODS

MB Preparation

Experiments were performed both in vivo and in vitro to determine whether MBs in skin significantly attenuate ultrasound transmission, thereby reducing petechiae bioeffects in underlying skeletal muscle. For these studies, MBs were prepared by sonicating a 1% solution of serum albumin in normal saline that was covered by a layer of octafluoro-propane gas (Flura, Newport, TN) as previously described.[15] MBs were counted and sized using a Multisizer Coulter Counter with negligible measurement error. Mean MB diameter was 2.63 μm with a standard deviation of 1.63 μm. Our MB formulation is similar to Optison (GE Healthcare), which is provided in concentrations of 5.0×10^8 to 8.0×10^8 MBs/mL and has a suggested maximum dose of 8.7 mL/patient. Assuming a patient weight of 80 kg, this dose scales to ~1×10^5 MBs/g, which was the baseline MB dose used in this study.

In Vivo Ultrasound Application

In vivo experiments were performed to determine the influence of [MB] and skin perfusion on petechiae bioeffects in underlying muscle. Animal studies were approved by the Institutional Animal Use and Care Committee. Sprague-Dawley rats were anesthetized by an intraperitoneal injection of ketamine (80 mg/kg) and xylazine (8 mg/kg). Mean animal weights ± standard deviation and the total number of rats per experimental group are presented in Table 1. The left jugular vein was cannulated with PE-50 gauge polyethylene tubing for MB injection. For experiments in which ultrasound was transmitted through unperfused skin, the skin directly above the gracilis muscle was surgically resected without disturbing the vasculature of the underlying gracilis muscle. The resected skin was then immediately returned to its in situ position without re-establishing vascular connections to the animal. Care was taken to ensure that no air bubbles were trapped under the resected skin. For experiments in which ultrasound was transmitted through perfused skin, the skin was not surgically manipulated. A water-based ultrasound gel (Parker Laboratories Aquasonic 100; Parker Laboratories, Inc., Fairfield, NJ) was applied to the perfused or unperfused skin above the gracilis muscle, and a 0.75″ diameter 1 MHz unfocused transducer (A314S; Panametrics, Waltham, MA) was coupled to the skin as shown in Figure 1. To reduce the potential for standing ultrasound waves, the dorsal hindlimb surface was coupled to a plastic stage. In some bolus injection studies, a 6.3-cm ultrasound transparent offset was placed between the skin and the transducer so that the hindlimb adductors were in the far field of the ultrasound beam. MBs (1×10^5, 2×10^5, or 3×10^5 MBs/g body

weight in 1 mL of 0.9% saline) were injected intravenously (I.V.) either as a bolus or as a continuous infusion with a pump (Harvard Apparatus PHD 2000; Harvard Apparatus, Holliston, MA) for the entire duration of the experiment. A total of 12 ultrasound pulses were applied. Ultrasound application time ranged from 2 minutes, which yielded a pulsing interval of 10 seconds, to 12 minutes, which yielded a pulsing interval of 1 minute. Each ultrasound pulse lasted 0.1 millisecond and consisted of 100 consecutive 1 MHz sinusoids of 1V peak-to-peak amplitude from a waveform generator (AFG-310; Tektronix, Inc., Beaverton, OR). The waveform signal was amplified by a 55 dB RF power amplifier (ENI 3100LA; Electronic Navigation Industries, Richardson, TX). These ultrasound pulsing parameters were based on previous therapeutic studies in which ultrasonic MB destruction was used to generate arteriogenesis[13–15] and the delivery of intravascular nanoparticles to muscle.[26] Based on in vitro hydrophone studies described in a forthcoming section, we estimate a peak-negative acoustic pressure of 1.18 MPa in the gracilis muscle in the absence of MBs. Previous studies have shown that, in the absence of MBs, petechiae are not created under these conditions,[26] so we did not designate an additional control group to receive ultrasound in the absence of MBs.

In Vivo Quantification of Petechiae Bioeffects

Muscles were inspected before ultrasound application to ensure that the surgical procedures did not create petechiae or leave blood smears on the muscle that could appear as petechiae. After the application of ultrasound, gracilis muscles were exposed and examined in their in situ configuration using a macroscope (Wild Makroskop Model 420; Wild, Heerbrugg, Switzerland) at 4× magnification. Color images were acquired using a digital camera (Olympus MicroFire S99809; Olympus Optical, Tokyo, Japan) and used to count discrete petechiae bioeffects.

In Vitro Peak-Negative Acoustic Pressure Measurements

To quantify how MB solutions attenuate the transmission of 1 MHz ultrasound, a gently stirred 5 mm thick ultrasound transparent chamber with a volume of 16 mL was placed in a tank containing degassed water and aligned between a 1 MHz unfocused ultrasound transducer (0.75″ diameter) and a 12 mm diameter hydrophone (HGL-0085; Specialty Engineering Associates, Sunnyvale, CA) as shown in Figure 2. The hydrophone, which was calibrated by the manufacturer, was placed in the near-field region to appropriately simulate ultrasound transmission to the gracilis muscle in vivo (Fig. 1). However, far field (ie, 6.3 cm between transducer and hydrophone) measurements were also made to verify that ultrasound attenuation was not near-field specific. For each experiment, the chamber was first filled with 0.9% saline solution, a single ultrasound pulse was applied, and baseline hydrophone measurements were made. As in the in vivo experiments, a single ultrasound pulse consisted of 100 consecutive 1 MHz sinusoids, the applied peak-to-peak voltage from the waveform generator was 1V, and the signal was amplified by 55 dB. After these initial measurements, the 0.9% saline solution was replaced with 0.9% saline solutions containing MBs in a range of concentrations, and hydrophone measurements were repeated. While in vivo MB dosages were based on animal body weight, [MB] in vitro was based on the weight of the fluid in the chamber (ie, 16 g = 16 mL of fluid with a density of 1 g/mL). Mean peak-negative pressure values were calculated by averaging peak-negative pressures from each of the 100 consecutive sinusoids within each individual pulse.

Statistics

For the bolus injection and 2 minutes continuous infusion groups, unpaired Student *t* tests were used. For the 12 minutes continuous injection groups, 1-way analysis of variance and pairwise comparisons with Tukey's *t* tests were used to test for differences within the unperfused and

perfused skin groups. Unpaired Student *t* tests were used to test for differences between unperfused and perfused skin groups at each MB dosage.

RESULTS

To determine whether skin perfusion affects the creation of petechiae bioeffects in underlying skeletal muscle, petechiae bioeffects were counted after bolus intravenous MB injection (1×10^5 MBs/g) and the application of 12 ultrasound pulses through perfused and unperfused skin over 2 minutes. Figure 3A and B illustrate that applying ultrasound through unperfused skin (Fig. 3B) leads to a marked increase in petechiae bioeffects, which appear as red spots and are denoted with arrows, when compared with the perfused skin group (Fig. 3A). Quantification of this response reveals that applying ultrasound through unperfused skin results in a 30-fold increase in petechiae bioeffects per unit surface area of muscle (Fig. 3C). In addition, we repeated these experiments with an offset that positioned the gracilis muscle in the far field of the ultrasound transducer. This experiment yielded essentially the same results, illustrating that the difference in petechiae creation between the perfused and unperfused skin groups was not due to near-field aberrations.

We then tested whether this perfusion-dependent phenomenon still occurs when MBs (1×10^5 MBs/g) are continuously injected to yield a lower time-averaged systemic MB concentration. Here, we injected MBs continuously over a 2-minute time period but kept the ultrasound pulsing protocol the same (ie, 12 pulses applied over 2 minutes). With this protocol, a 3.5-fold increase in petechiae bioeffects was observed for the unperfused skin group (Fig. 4), indicating that petechiae bioeffects are still diminished when MBs are slowly infused into the circulation.

While the results in Figure 3 and Figure 4 show that skin perfusion inhibits petechiae formation in underlying muscle, they do not indicate whether this effect was caused by blood constituents and/or circulating MBs in the skin. To address this question, we developed a protocol in which 1 ultrasound pulse was applied per min over 12 minutes while MBs were continuously injected at different concentrations (1×10^5, 2×10^5, or 3×10^5 MBs/g). At the lowest MB dosage (1×10^5 MBs/g), there was no significant difference between the perfused and unperfused skin groups. However, increasing MB dosage to 2×10^5 MBs/g (ie, 2-fold above the lowest dosage) elicited an approximately 1.5-fold increase in petechiae bioeffects for the unperfused skin groups (Fig. 5). Likewise, a 3-fold increase in MBs/g (ie, from 1×10^5 to 3×10^5 MBs/g) caused a 2.4-fold increase in petechiae bioeffects. However, when the overlying skin remained perfused, these same 2- and 3-fold increases in MB dose led to statistically significant 60% and 75% decreases in petechiae bioeffects, respectively. Petechiae bioeffects/mm^2 was significantly greater for the unperfused skin group at both 2×10^5 and 3×10^5 MBs/g. These results indicate that the presence of MBs in the skin overlying the gracilis muscle was responsible for inhibiting petechiae.

Finally, we tested the hypothesis that MBs in the skin inhibit petechiae by attenuating ultrasound transmission. To this end, we made hydrophone measurements of ultrasound transmission through solutions containing MBs at different concentrations (Fig. 6). In Figure 6, mean peak-negative pressure per ultrasound pulse is shown over the entire range of tested [MB]s and fit with an exponential decay regression function. Peak-negative pressure is a maximum when no MBs are present in the fluid. As [MB] is raised, ultrasound transmission becomes attenuated and peak-negative pressure falls rapidly. At 1×10^5 MBs/mL, peak-negative pressure is reduced by 65% from MB-free control (ie, to 0.4 MPa). Ultrasound is no longer detectable at a [MB] of 6×10^5 MBs/g. In the far-field, at concentrations $<0.1 \times 10^5$ MBs/mL, absolute peak-negative pressures are greater than for the near-field (Fig. 6). However, at concentrations $>1.0 \times 10^5$ MBs/mL, far-field and near-field pressures become

virtually identical, indicating that the acoustic attenuation created by MBs is even more significant in the far-field.

DISCUSSION

Acoustic Attenuation and Petechiae Bioeffect Creation

Our central finding is that acoustic attenuation by MBs in superficial tissue has an unexpectedly significant impact on the creation of petechiae in deep tissue. We manipulated [MB] in a superficial tissue by resecting the skin between the ultrasound transducer and the underlying muscle of interest and then immediately replacing the skin without re-establishing vascular connections. With this approach, on bolus MB injection, we observed a 30-fold increase in petechiae when skin perfusion was eliminated (Fig. 3). Virtually identical results were achieved in far-field experiments, illustrating that this effect was not near-field specific. To insure that this phenomenon was not specific to bolus injections, we also performed continuous injections over a period of 2 minutes (Fig. 4). While differences in petechiae between perfused and unperfused skin were not as pronounced with continuous injection, a statistically significant 3.5-fold increase in petechiae was still observed in the absence of skin perfusion.

Because the unperfused skin remained in the ultrasound path, the experiments in Figure 3 and Figure 4 isolated petechiae inhibition to the skin perfusate and not the skin tissue itself. However, it was possible that skin blood flow could have affected petechiae bioeffect attenuation independent of the presence of MBs. Therefore, to isolate the influence of MBs, we altered MB dosage without changing skin blood flow (Fig. 5). Here, a 3-fold increase in circulating [MB] created a 75% decrease in petechiae, indicating that MBs in the skin are primarily responsible for petechiae attenuation. In addition, in the absence of acoustic attenuation by MBs, the creation of petechiae is approximately proportional to [MB] in this range of MB doses (Fig. 5).

Interestingly, comparing the results in Figure 4 with the low dose (ie, 1×10^5 MBs/g) group in Figure 5 indicates that either pulsing interval or total experimental duration had an influence on petechiae creation. This is because, even though both MB concentration (1×10^5 MBs/g) and total applied ultrasound (12 pulses) were equivalent for these groups, petechiae/mm^2 for both the unperfused and perfused cases seems to be quite different. Since only pulsing interval and total experimental duration differ between these 2 protocols, we can isolate this difference to 1 of these 2 factors. Of these 2 factors, it is unlikely that pulsing interval was responsible for 2 reasons. First, previous studies[26] indicate that a pulsing interval of 10 seconds will permit a complete refresh of MB concentration after a MB-destructive pulse in rat skeletal muscle under conditions of normal tone. Second, the data actually suggest that there are more MBs present in the muscle when using the shorter pulse interval (10 seconds; Fig. 4) as opposed to the longer interval (1 minute; Fig. 5), which is exactly the opposite of what we would expect if the 10-second interval were too short. For these reasons, we believe that the difference in total duration must be the key factor responsible for the discrepancies. The use of a longer total duration in Figure 5 (ie, 12 minutes) most likely caused a time-averaged reduction in MB concentration in the systemic circulation because there was more time for MB deflation and/or MB sequestration into the liver and lungs to occur. Such a decrease in MB concentration would appear as a decrease in petechiae in the unperfused skin group, due to fewer MBs being available to create petechiae, and an increase in petechiae in the perfused group, due to fewer MBs in the skin being available to attenuate ultrasound. Indeed, this is exactly what we observed in the low dose group of Figure 5 when compared with Figure 4.

We can estimate the mathematical relationship between petechiae bioeffect attenuation and [MB] based on any increment in MB dose in Figure 5. The ratio of petechiae at some high MB dose to petechiae at a lower MB dose in the perfused skin group (R_p) equates to the ratio of

petechiae amplification in muscle to petechiae attenuation in skin, where both the amplification and attenuation terms are dependent on [MB]. Petechiae amplification in muscle is simply the same ratio for the unperfused skin group (R_u) because petechiae bioeffect attenuation by skin is absent under these conditions. From these 2 ratios, we can then calculate petechiae attenuation as R_u/R_p and determine petechiae attenuation as a function of the change in [MB] for a given MB dosage increment. We express the dependence of petechiae attenuation (R_u/R_p) on [MB] to an unknown power, x (Eq. 1).

$$\left(\frac{[\mathrm{MB_{Hi}}]}{[\mathrm{MB_{Lo}}]}\right)^X = \frac{R_u}{R_P} \tag{1}$$

In Table 2, the exponent "x" is calculated for each of the 3 [MB] increments, ranging from 1.89 to 2.39 with a mean of 2.1. Therefore, we estimate that petechiae attenuation in skin is approximately dependent on $[MB]^{2.1}$. Establishing a more precise relationship would require additional groups; nevertheless, under these conditions, it is clear that petechiae attenuation by skin dominates petechiae amplification in muscle.

Hydrophone measurements (Fig. 6) were made to determine how MBs attenuate ultrasound transmission and, in turn, possibly inhibit petechiae in vivo. By making the assumption that in vivo MB dosage directly scales to local [MB] in skin implies that a [MB] of 1×10^5 MBs/g in the skin is simulated in vitro by the 1×10^5 MBs/mL data point in Figure 6. Because a solution with 1×10^5 MBs/mL reduces peak negative pressure from 1.18 MPa to 0.40 MPa (ie, ~65%), we estimate that an intravenously administered bolus injection of 1×10^5 MBs/g will also reduce peak-negative pressure in underlying muscle by ~65%. Indeed, studies by other investigators confirm that MBs in the diameter and concentration ranges studied here markedly attenuate ultrasound transmission.[30–34] Furthermore, in addition to being dependent on frequency[30–32] and power,[32] studies using trapped[30,31] and suspended[33] MBs are consistent with our observations (Fig. 6) and illustrate that attenuation is exponentially dependent on [MB].

In Figure 3, a bolus MB injection generated a 30-fold decrease in petechiae when ultrasound was applied through perfused skin. Qin and Ferrara[27] predicted that circumferential microvessel wall stresses created by MB expansion at 1 MHz are reduced more than 2-orders of magnitude, to a level that is below a critical threshold for microvessel rupturing, when peak-negative pressure is decreased by 60%. Although the range and absolute magnitude of peak-negative pressures explored by Qin and Ferrara[27] were less than those measured here, both studies support the hypothesis that a 60% to 65% reduction in peak-negative pressure can exert a disproportionately large influence on bioeffect creation. Ultimately, we believe that this is the most likely mechanism through which acoustic attenuation exerts its strong inhibitory influence on petechiae bioeffect creation.

Comparisons to Other In Vivo Studies

We chose to test the influence of MBs in superficial tissue on petechiae creation in deep tissue using a rat hind-limb skin resection model because the surgical intervention does not sever vascular connections between the skin and the muscle, thereby leaving blood flow to the underlying muscle relatively unaffected. Although we only studied attenuation by MBs in skin, it is probable that our conclusions are relevant for other tissues and organs. Indeed, because skin blood volume in the rat is relatively low in comparison to other tissues and organs,[35] other superficial tissues are likely to generate even greater MB-induced attenuation. Our results (Fig. 5) are generally consistent with other studies which report that, at low MB doses, petechiae and MB dosage are proportional in muscle and intestine,[19] and in the heart, MB dose is

proportional to myocyte injury and premature heart beats.[24] However, at higher MB doses, bioeffects tend to approach a maximum or even decline.[24] One explanation has been that several petechiae can merge and may appear as individual petechiae when they become numerous.[19] Our findings suggest that attenuation by MBs provides another possible explanation. Because petechiae inhibition by acoustic attenuation is so strongly dependent on [MB] at high MB dosages, it will eventually dominate the system and cause petechiae to reach a maximum limit and eventually decrease.

Implications for Contrast Ultrasound Safety and Therapeutics

While there are many reports indicating that contrast agent MBs have accrued an excellent safety record,[36–38] the Food and Drug Administration has recently requested labeling changes on Optison and Definity in response to complications in some patients. Although the topic of our study was MB-induced bioeffects, it is important to emphasize that our results should have relatively little bearing on these current discussions of contrast agent safety. Indeed, the ability of contrast ultrasound to create petechiae in mice,[19] rats,[20,24] rabbits,[18] and dogs[22] is well-known; however, it is unclear whether small animals can accurately reflect human responses.[39] Thus, it is difficult to ascertain whether, at this time, our results are directly applicable to humans. Furthermore, we note that our ultrasound parameters were based on protocols for therapeutic MB destruction and are unlike those routinely used in the clinic for diagnostic imaging. These differences in ultrasound parameters could have a significant bearing on the applicability of this study to the clinic.

In contrast, we do believe these results have significant implications for the design of emerging contrast ultrasound-based therapeutics that require microvessel permeabilization with low frequency and/or high power ultrasound. To date, ultrasound targeted drug and gene delivery strategies have been optimized primarily through modifications to ultrasound pulsing interval, MB injection site, and agent composition.[26,40] Our results indicate that, for delivery to deep tissues, MB dose and/or injection time should also be carefully considered. In general, for scenarios in which the number of petechiae bioeffects correlates with the efficacy of treatment,[15] petechiae bioeffect creation can be enhanced by using lower MB dosages and/or increasing the total time of MB injection and ultrasound application.

Limitations of the Study

Although our results indicate that the attenuation of ultrasound by MBs in a superficial tissue can diminish petechiae bioeffects in deep tissue, these results should be interpreted carefully due to some limitations in our study. First, because there are no direct vascular connections between the skin over the gracilis muscle and the gracilis muscle itself, we proposed that gracilis muscle blood flow was not significantly affected by removing the overlying skin. However, gracilis muscle blood flow was not explicitly measured after skin removal, so it is possible that local MB concentration in the gracilis muscle was affected somewhat by the procedure. Second, it is important to emphasize that the value of the exponent in Eq. 1 was estimated using only 3 groups. It is entirely possible that the addition of more groups to the study would yield a different value for this exponent or even indicate that this relationship shows better agreement when fit to a different mathematical form. Third, to facilitate comparison of the in vitro data in Figure 6 with the in vivo data in Figure 3, we had to assume that [MB] in skin is representative of [MB] throughout the whole animal. Skin blood flow and volume are regulated by vascular tone which, in turn, is affected by temperature, depth of anesthesia, and many other factors. Therefore, it is possible that the quality of this assumption varied from animal to animal. Finally, in the in vitro studies of Figure 6, the MB chamber thickness was chosen to mimic the in vivo distance between the transducer and the gracilis muscle. However, this approach did not account for any absolute ultrasound attenuation created by the skin tissue itself. While we would not expect the addition of an unperfused piece of skin

to the ultrasound path to appreciably change the shape of the curve in Figure 6, which is the key piece of evidence suggesting that ultrasound attenuation in the skin reduced peak-negative pressure in the muscle to a value below the microvessel rupturing threshold, we would expect this intervention to cause the entire curve to exhibit a slight but relatively uniform downward shift.

Acknowledgments

Supported by AHA Grant-In-Aid 0555511U and NIH R01 HL74082.

REFERENCES

1. Hom BK, Shrestha R, Palmer SL, et al. Prospective evaluation of vascular complications after liver transplantation: comparison of conventional and microbubble contrast-enhanced ultrasound. Radiology 2006;241:267–274. [PubMed: 16990679]
2. Dai Y, Chen MH, Yin SS, et al. Focal liver lesions: can Sonovue-enhanced ultrasound be used to differentiate malignant from benign lesions? Invest Radiol 2007;42:596–603. [PubMed: 17620943]
3. Watanabe R, Matsumura M, Munemasa T, et al. Mechanism of hepatic parenchyma-specific contrast of microbubble-based contrast agent for ultrasonography: microscopic studies in the liver. Invest Radiol 2007;42:643–651. [PubMed: 17700280]
4. Weber MA, Krix M, Jappe U, et al. Pathologic skeletal muscle perfusion in patients with myositis: detection with quantitative contrast-enhanced US—initial results. Radiology 2005;238:640–649. [PubMed: 16371585]
5. Wei K, Jayaweera AR, Firoozan S, et al. Quantification of myocardial blood flow with ultrasound-induced destruction of microbubbles administered as a constant venous infusion. Circulation 1998;97:473–483. [PubMed: 9490243]
6. Bekeredjian R, Chen S, Frenkel PA, et al. Ultrasound-targeted micro-bubble destruction can repeatedly direct highly specific plasmid expression to the heart. Circulation 2003;108:1022–1026. [PubMed: 12912823]
7. Kondo I, Ohmori K, Oshita A, et al. Treatment of acute myocardial infarction by hepatocyte growth factor gene transfer: the first demonstration of myocardial transfer of a “functional” gene using ultrasonic microbubble destruction. J Am Coll Cardiol 2004;44:644–653. [PubMed: 15358035]
8. Shohet RV, Chen S, Zhou YT, et al. Echocardiographic destruction of albumin microbubbles directs gene delivery to the myocardium. Circulation 2000;101:2554–2556. [PubMed: 10840004]
9. Taniyama Y, Tachibana K, Hiraoka K, et al. Development of safe and efficient novel nonviral gene transfer using ultrasound: enhancement of transfection efficiency of naked plasmid DNA in skeletal muscle. Gene Ther 2002;9:372–380. [PubMed: 11960313]
10. Christiansen JP, French BA, Klibanov AL, et al. Targeted tissue transfection with ultrasound destruction of plasmid-bearing cationic microbubbles. Ultrasound Med Biol 2003;29:1759–1767. [PubMed: 14698343]
11. Lu QL, Liang HD, Partridge T, et al. Microbubble ultrasound improves the efficiency of gene transduction in skeletal muscle in vivo with reduced tissue damage. Gene Ther 2003;10:396–405. [PubMed: 12601394]
12. Mukherjee D, Wong J, Griffin B, et al. Ten-fold augmentation of endothelial uptake of vascular endothelial growth factor with ultrasound after systemic administration. J Am Coll Cardiol 2000;35:1678–1686. [PubMed: 10807476]
13. Song J, Qi M, Kaul S, et al. Stimulation of arteriogenesis in skeletal muscle by microbubble destruction with ultrasound. Circulation 2002;106:1550–1555. [PubMed: 12234963]
14. Song J, Cottler PS, Klibanov AL, et al. Microvascular remodeling and accelerated hyperemia blood flow restoration in arterially occluded skeletal muscle exposed to ultrasonic microbubble destruction. Am J Physiol Heart Circ Physiol 2004;287:H2754–H2761. [PubMed: 15319212]
15. Chappell JC, Klibanov AL, Price RJ. Ultrasound-microbubble-induced neovascularization in mouse skeletal muscle. Ultrasound Med Biol 2005;31:1411–1422. [PubMed: 16223645]

16. Imada T, Tatsumi T, Mori Y, et al. Targeted delivery of bone marrow mononuclear cells by ultrasound destruction of microbubbles induces both angiogenesis and arteriogenesis response. Arterioscler Throm Vasc Biol 2005;25:2128–2134.
17. Yoshida J, Ohmori K, Takeuchi H, et al. Treatment of ischemic limbs based on local recruitment of vascular endothelial growth factor-producing inflammatory cells with ultrasonic microbubble destruction. J Am Coll Cardiol 2005;46:899–905. [PubMed: 16139142]
18. Ay T, Havaux X, Van Camp G, et al. Destruction of contrast microbubbles by ultrasound: effects on myocardial function, coronary perfusion pressure, and microvascular integrity. Circulation 2001;104:461–466. [PubMed: 11468210]
19. Miller DL, Quddus J. Diagnostic ultrasound activation of contrast agent gas bodies induces capillary rupture in mice. Proc Natl Acad Sci U S A 2002;97:10179–10184. [PubMed: 10954753]
20. Skyba DM, Price RJ, Linka AZ, et al. Direct in vivo visualization of intravascular destruction of microbubbles by ultrasound and its local effects on tissue. Circulation 1998;98:290–293. [PubMed: 9711932]
21. Price RJ, Skyba DM, Kaul S, et al. Delivery of colloidal particles and red blood cells to tissue through microvessel ruptures created by targeted microbubble destruction with ultrasound. Circulation 1998;98:1264–1267. [PubMed: 9751673]
22. Miller DL, Driscoll EM, Dou C, et al. Microvascular permeabilization and cardiomyocyte injury provoked by myocardial contrast echocardiography in a canine model. J Am Coll Cardiol 2006;47:1464–1468. [PubMed: 16580537]
23. Shohet RV, Grayburn PA. Potential bioeffects of ultrasonic destruction of microbubble contrast agents. J Am Coll Cardiol 2006;7:1469–1470. [PubMed: 16580538]
24. Miller DL, Li P, Dou C, et al. Influence of contrast agent dose and ultrasound exposure on cardiomyocyte injury induced by myocardial contrast echocardiography in rats. Radiology 2005;237:137–143. [PubMed: 16183929]
25. Vancraeynest D, Kefer J, Hanet C, et al. Release of cardiac biomarkers during high mechanical index contrast-enhanced echocardiography in humans. Eur Heart J 2007;28:1236–1241. [PubMed: 17409107]
26. Song J, Chappell JC, Qi M, et al. Influence of injection site, microvascular pressure and ultrasound variables on microbubble-mediated delivery of microspheres to muscle. J Am Coll Cardiol 2002;39:726–731. [PubMed: 11849875]
27. Qin S, Ferrara KW. Acoustic response of compliable microvessels containing ultrasound contrast agents. Physics Med Biol 2006;51:5065–5088.
28. Porter TR, Xie F. Transient myocardial contrast after initial exposure to diagnostic ultrasound pressures with minute doses of intravenously injected microbubbles: demonstration and potential mechanisms. Circulation 1995;92:2391–2395. [PubMed: 7586336]
29. Forsberg F, Liu JB, Shi WT, et al. In vivo perfusion estimation using subharmonic contrast microbubble signals. J Ultrasound Med 2006;25:15–21. [PubMed: 16371551]
30. Wu J, Nyborg WL. Measurements of frequency spectra of transmission coefficients to ultrasound through trapped microbubbles. Ultrasonics 1990;28:115–199. [PubMed: 2309376]
31. Miller DL. Experimental investigation of the response of gas-filled micropores to ultrasound. J Acoust Soc Am 1982;71:471–476.
32. Tang MX, Eckersley RJ. Frequency and pressure dependent attenuation and scattering by microbubbles. Ultrasound Med Biol 2007;33:164–168. [PubMed: 17189060]
33. Marsh JN, Hughes MS, Hall CS, et al. Frequency and concentration dependence of the backscatter coefficient of the ultrasound contrast agent Albunex®. J Acoust Soc Am 1998;104:1654–1666.
34. Casciaro S, Errico RP, Conversano F, et al. Experimental investigations of nonlinearities and destruction mechanisms of an experimental phospholipids-based ultrasound contrast agent. Invest Radiol 2007;42:95–104. [PubMed: 17220727]
35. Everett NB, Simmons B, Lasher EP. Distribution of blood (Fe59) and plasma (I131) volumes of rats determined by liquid nitrogen freezing. Circ Res 1956;4:419–424. [PubMed: 13330185]
36. Jakobsen JA, Oyen R, Thomsen HS, et al. Safety of ultrasound contrast agents. Eur Radiol 2005;15:941–945. [PubMed: 15662495]

37. Borges AC, Walde T, Reibis RK, et al. Does contrast echocardiography with Optison induce myocardial necrosis in humans? J Am Soc Echocardiogr 2002;15:1080–1086. [PubMed: 12373250]

38. Knebel F, Schimke I, Eddicks S, et al. Does contrast echocardiography induce increases in markers of myocardial necrosis, inflammation, and oxidative stress suggesting myocardial injury? Cardiovasc Ultrasound 2005;3:21. [PubMed: 16107209]

39. Sahn DJ. Arrhythmias in rat hearts exposed to pulsed ultrasound after intravenous injection of a contrast agent. J Ultrasound Med 2002;21:1343–1345.

40. Chen S, Shohet RV, Bekeredjian R, et al. Optimization of ultrasound parameters for cardiac gene delivery of adenoviral or plasmid deoxyribonucleic acid by ultrasound-targeted microbubble destruction. J Am Coll Cardiol 2003;42:301–308. [PubMed: 12875768]

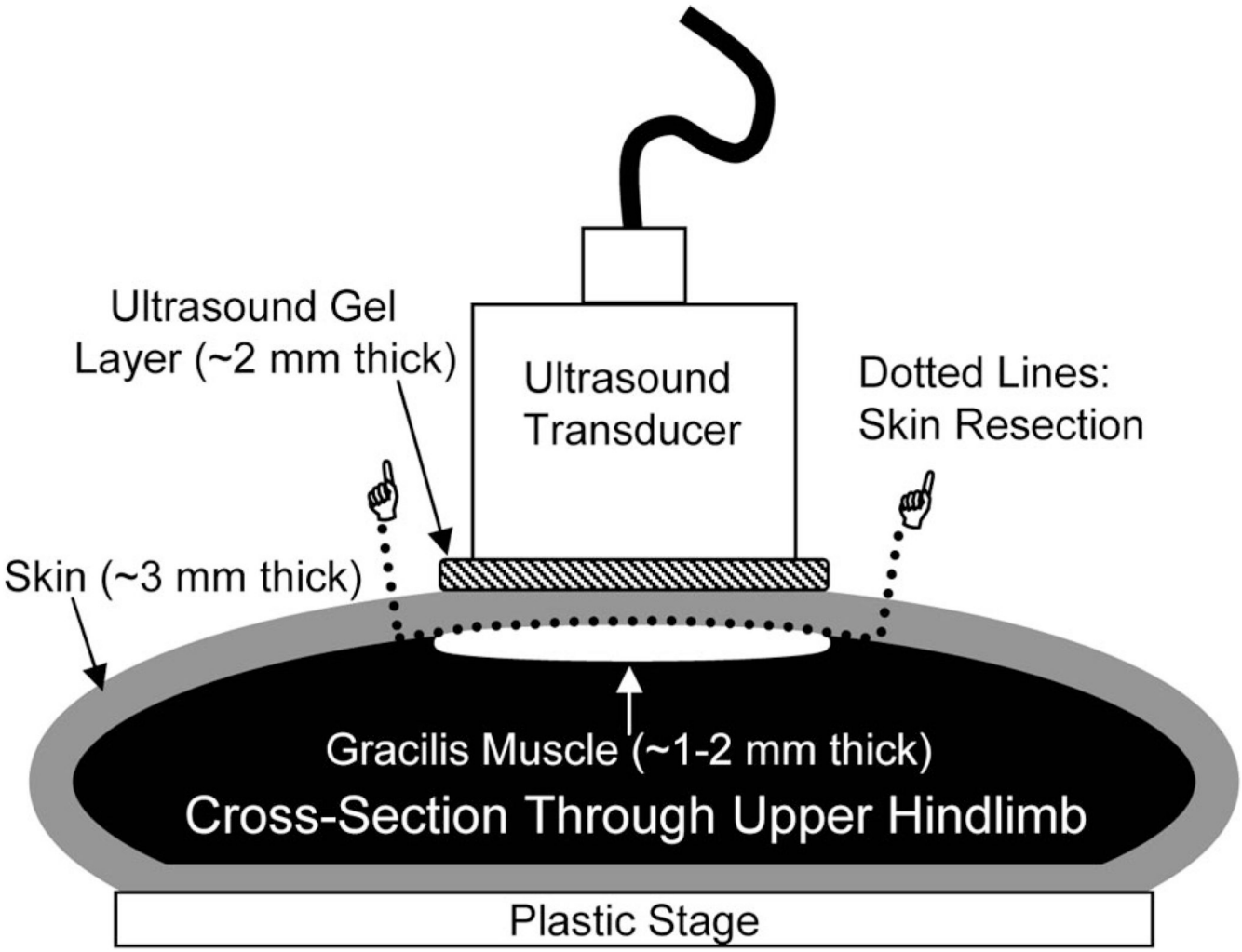

FIGURE 1.

Schematic cross-section of a rat upper hindlimb showing how the ultrasound transducer was positioned with respect to the resected skin patch and the underlying gracilis muscle during the in vivo experiments. Note that the gracilis muscle lies directly beneath the resected skin. Approximate gel layer, skin, and muscle thicknesses are provided.

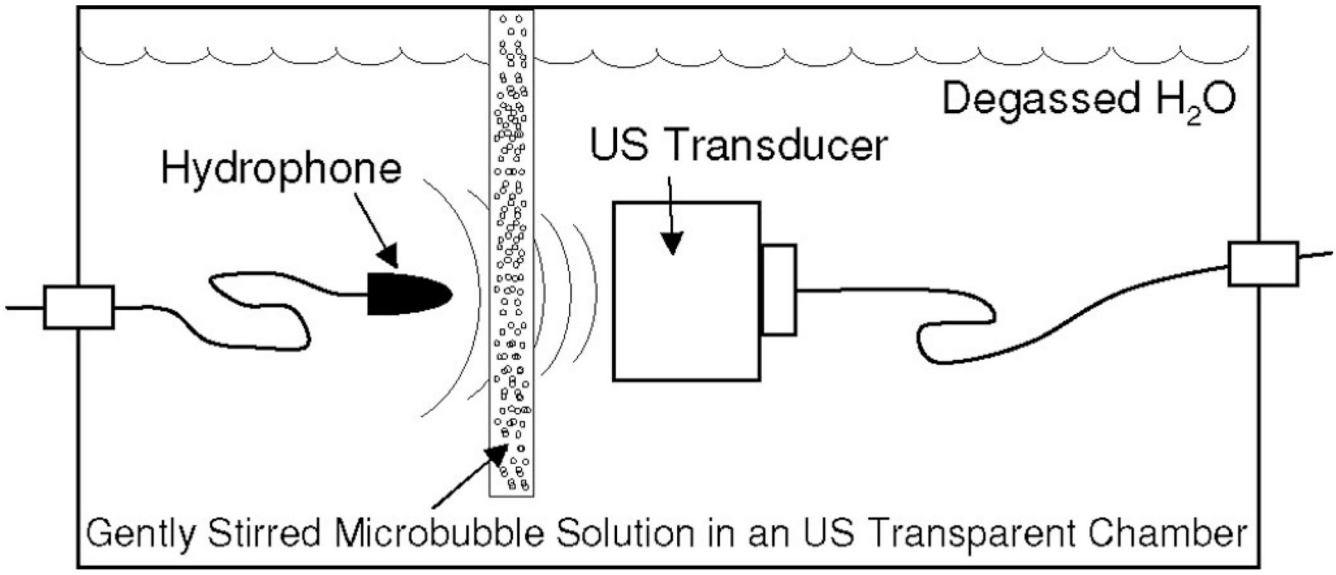

FIGURE 2.
Schematic illustration of the in vitro apparatus used for making hydrophone measurements of ultrasound transmission through solutions containing various [MB]s.

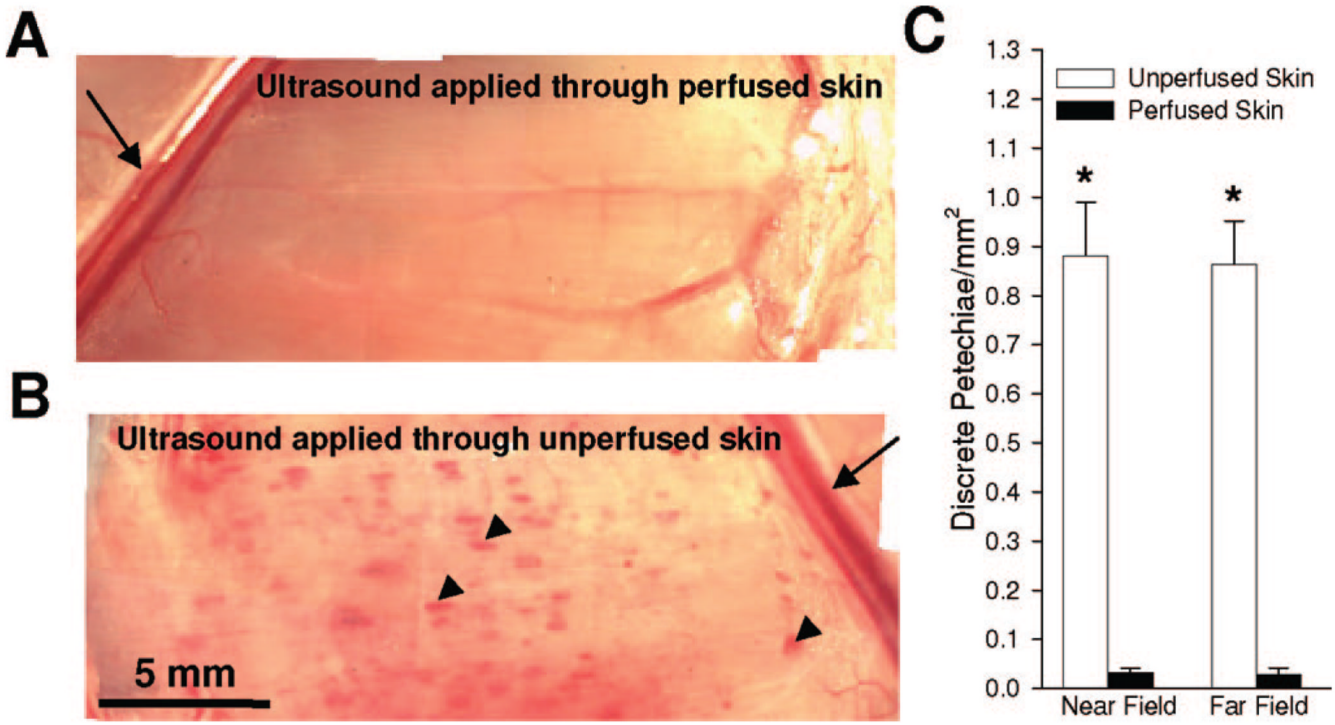

FIGURE 3.

Petechiae bioeffect creation in gracilis muscle after bolus injection of 1×10^5 MBs/g and near-field ultrasound application over 2 minutes. (A, B) En-face photomicrographs of gracilis muscles after ultrasound application through perfused (A) and unperfused skin (B). Note the significant increase in discrete petechiae bioeffects (arrows) when ultrasound is applied through unperfused skin. Arrows denote the saphenous artery and vein. Arrowheads denote discrete petechiae. (C) Bar graph showing petechiae bioeffects/ mm^2 when gracilis muscle is placed in either the near field or far field. *Significantly different ($P < 0.05$) than perfused skin in same group.

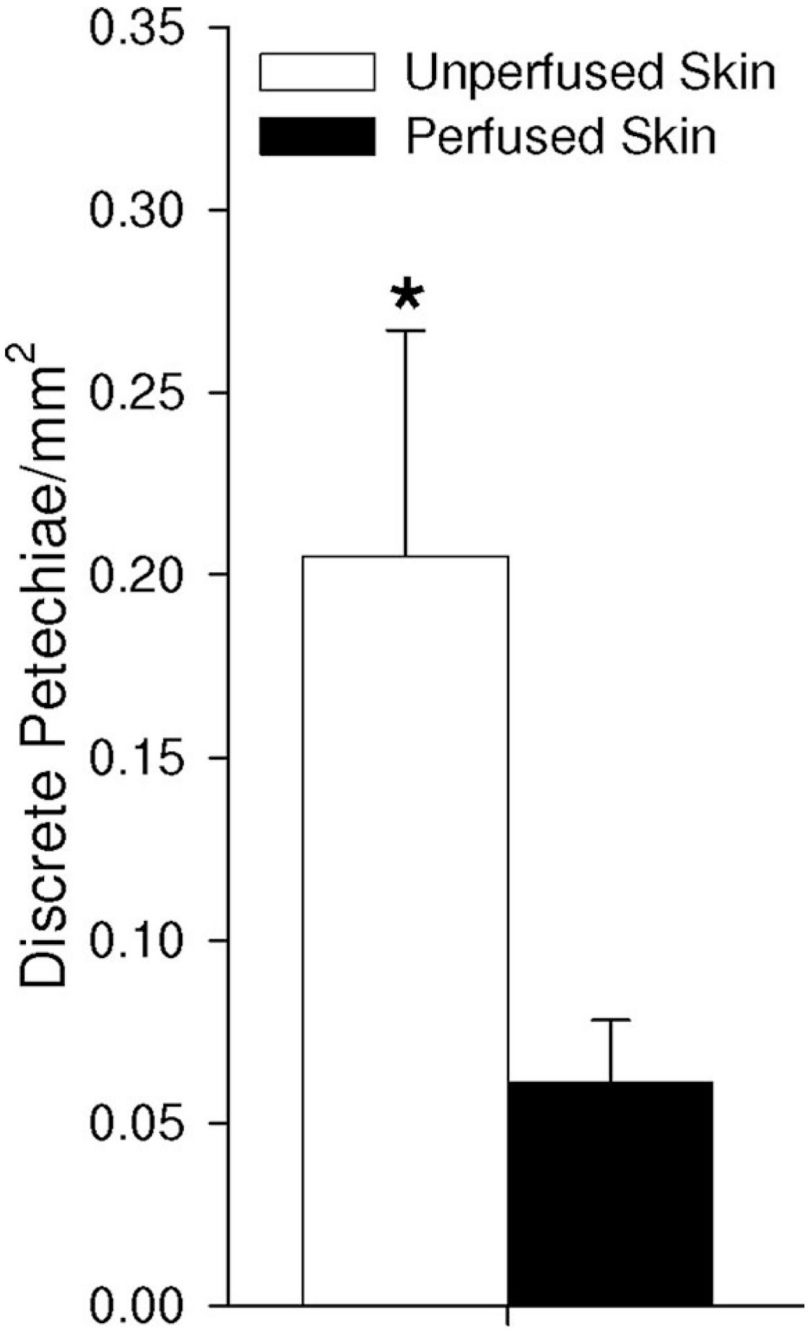

FIGURE 4.
Bar graph illustrating petechiae bioeffects/mm^2 in gracilis muscle when 1×10^5 MBs/g are injected over 2 minutes. *Significantly different ($P < 0.05$) than perfused skin group.

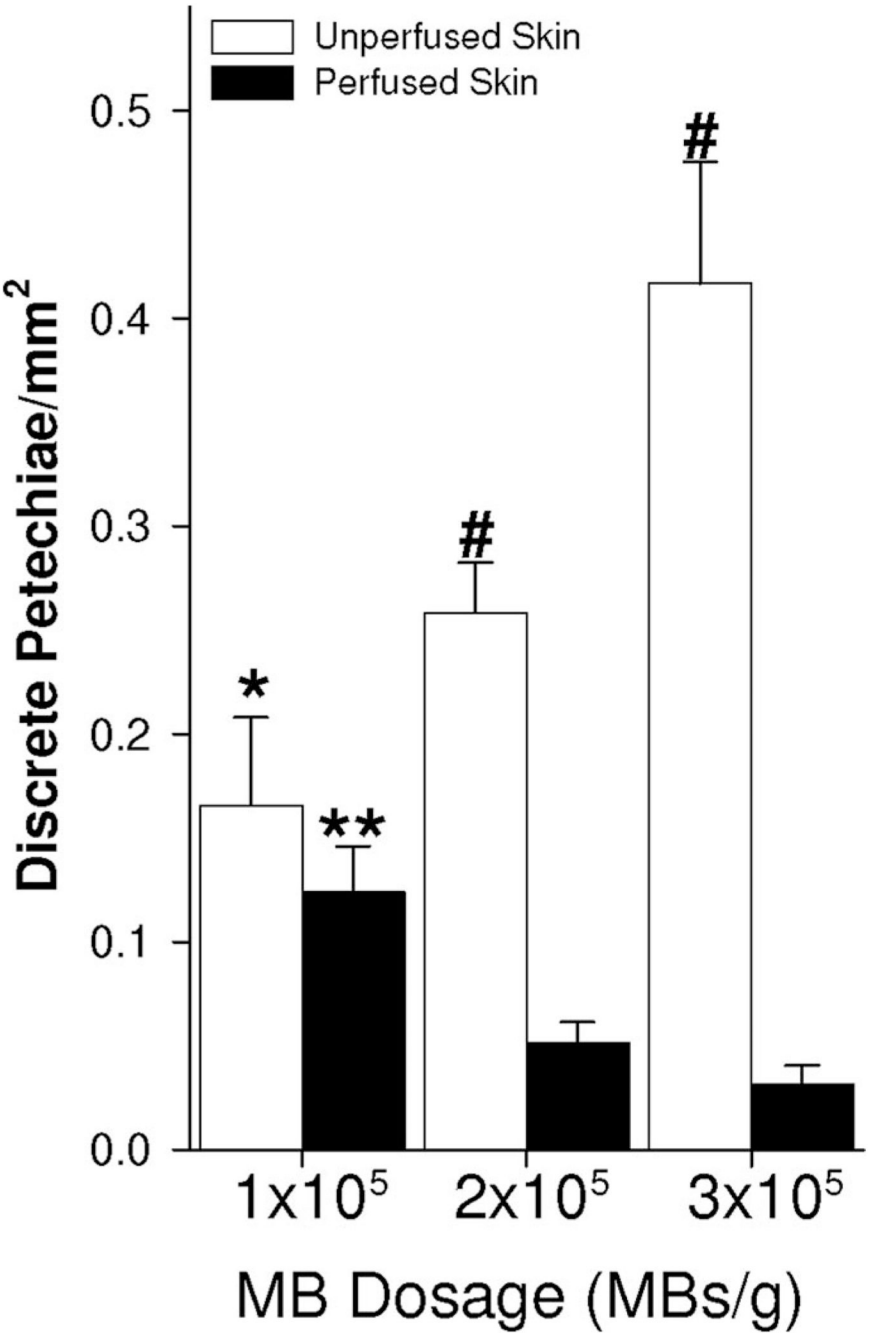

FIGURE 5.

Bar graph illustrating petechiae bioeffects/mm^2 during continuous injection of MBs at 1 × 10^5, 2 × 10^5, and 3 × 10^5 MBs/g over a period of 12 minutes. *Significantly different (P < 0.05) than unperfused group at 3 × 10^5 MBs/g. **Significantly different (P < 0.05) than perfused group at 2 × 10^5 and 3 × 10^5 MBs/g. #Significantly different (P < 0.05) than perfused group at same MB dosage.

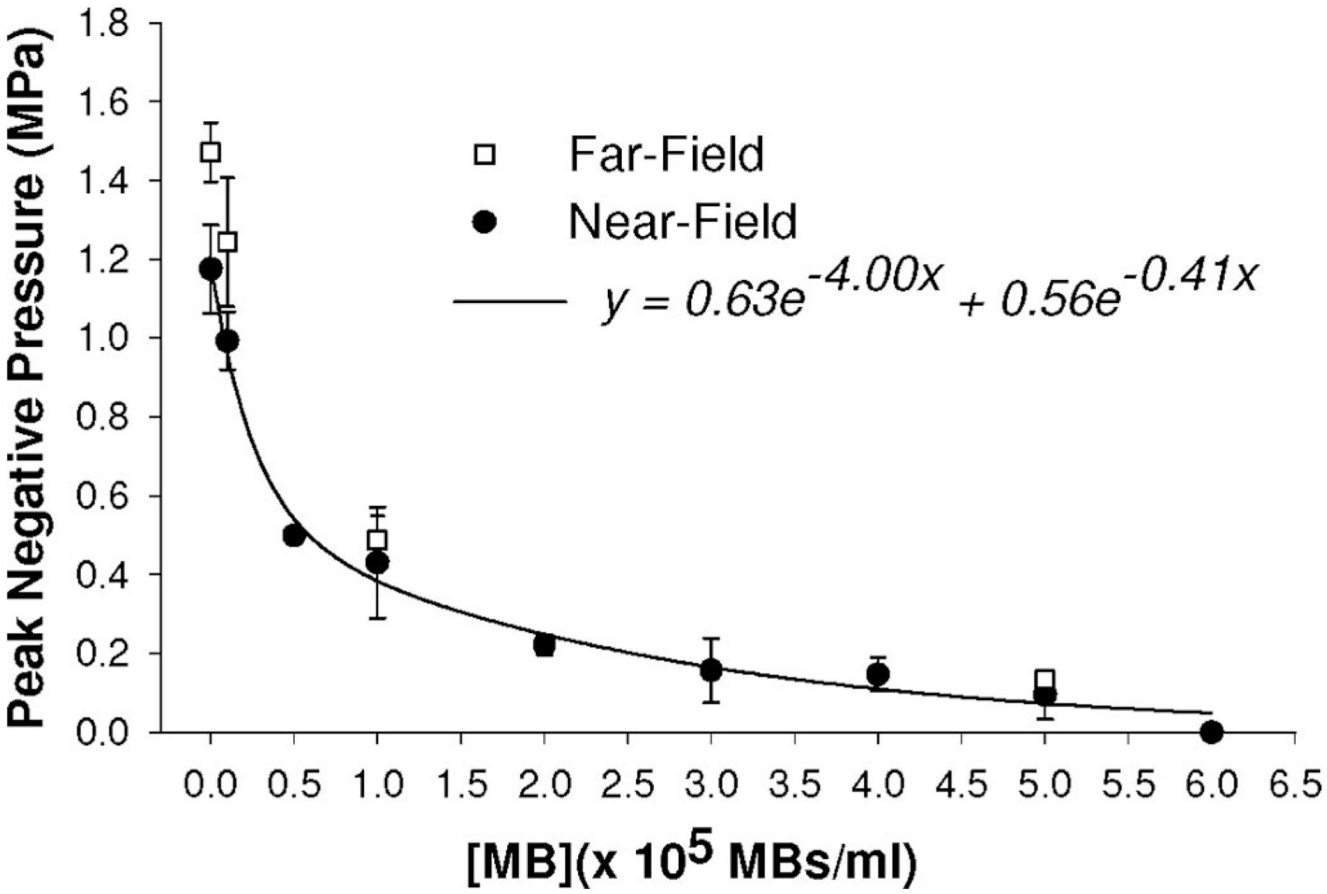

FIGURE 6.

Hydrophone measurements showing the mean peak-negative pressure of ultrasound transmitted through solutions containing MBs at various concentrations. Data are means ± standard deviation. Each data point is the mean of between 3 and 5 separate trials. Near-field data are fit with an exponential decay regression.

TABLE 1

Animal Weights and "n" Values for Each Experimental Group

Figure	InjectionTime (min)	Skin Perfusion	Near or Far Field	MB Dosage (MBs/g Body Weight)	"n"	Animal Body Weight (g ± SD)
3	Bolus	Perfused	Near	1×10^5	6	196.3 ± 6.8
	Bolus	Unperfused	Near	1×10^5	6	197.6 ± 7.3
	Bolus	Perfused	Far	1×10^5	4	209.3 ± 12.1
	Bolus	Unperfused	Far	1×10^5	5	219.1 ± 16.3
4	2	Perfused	Near	1×10^5	6	204.3 ± 8.0
	2	Unperfused	Near	1×10^5	6	207.6 ± 8.6
5	12	Perfused	Near	1×10^5	6	201.8 ± 8.0
	12	Unperfused	Near	1×10^5	6	210.2 ± 12.0
	12	Perfused	Near	2×10^5	6	217.6 ± 30.7
	12	Unperfused	Near	2×10^5	6	209.7 ± 27.5
	12	Perfused	Near	3×10^5	6	208.6 ± 8.0
	12	Unperfused	Near	3×10^5	6	213.4 ± 8.7

MB indicates microbubble.

TABLE 2

Parameters for Calculating Dependence of Petechiae Bioeffect Attenuation on Microbubble Conentration

MB Dose Increment (MBs/g)	Fold Increase in [MB]	R_p	R_u	R_u/R_p	X
1×10^5 to 3×10^5	3	0.26	2.50	9.62	2.06
1×10^5 to 2×10^5	2	0.42	1.56	3.71	1.89
2×10^5 to 3×10^5	1.5	0.61	1.61	2.64	2.39

MB indicates microbubble; [MB], microbubble concentration; R_p, ratio of petechiae bioeffects/mm^2 at higher MB dose to petechiae bioeffects/mm^2 at lower MB dose within perfused skin groups as shown in Figure 5; R_u, ratio of petechiae bioeffects/mm^2 at higher MB dose to petechiae bioeffects/mm^2 at lower MB dose within unperfused skin groups as shown in Figure 5; X, power to which petechiae bioeffect attenuation is dependent on Eq. 1.